# Using the Dipolar and Quadrupolar Moments to Improve Solar-Cycle Predictions Based on the Polar Magnetic Fields

Andrés Muñoz-Jaramillo*
*Harvard-Smithsonian Center for Astrophysics, Cambridge, Massachusetts 02138, USA*
*University Corporation for Atmospheric Research, Boulder, Colorado 80307, USA*
*Department of Physics & Astronomy, University of Utah, Salt Lake City, Utah 84112, USA*

Laura A. Balmaceda
*Institute for Astronomical, Terrestrial and Space Sciences (ICATE-CONICET), J5402DSP San Juan, Argentina*

Edward E. DeLuca
*Harvard-Smithsonian Center for Astrophysics, Cambridge, Massachusetts 02138, USA*
(Received 13 December 2012; published 26 July 2013)

The solar cycle and its associated magnetic activity are the main drivers behind changes in the interplanetary environment and Earth's upper atmosphere (commonly referred to as space weather and climate). In recent years there has been an effort to develop accurate solar cycle predictions, leading to nearly a hundred widely spread predictions for the amplitude of solar cycle 24. Here we show that cycle predictions can be made more accurate if performed separately for each hemisphere, taking advantage of information about both the dipolar and quadrupolar moments of the solar magnetic field during minimum.

DOI: 10.1103/PhysRevLett.111.041106 PACS numbers: 96.60.qd, 96.60.Q−

*Introduction.*—The solar magnetic cycle is a process that brings the global magnetic field of the Sun (back and forth) from a configuration that is predominantly poloidal (contained inside the meridional plane), to one predominantly toroidal (wrapped around the axis of rotation; locally perpendicular to the meridional plane). During the first part of this process (poloidal to toroidal field), the poloidal components of the magnetic field are stretched and amplified by solar differential rotation [1]. This forms belts of amplified toroidal field which are transported to low latitudes, become buoyantly unstable due to overshooting convection, and rise to the surface to form bipolar sunspot groups (BSGs) [2,3]. There are several mechanisms which may be playing a role during the second part of the process (toroidal to poloidal field) [4] and the main contending theory at present is commonly referred to as the Babcock-Leighton mechanism [5,6]: The fact that BSGs present a systematic tilt with respect to a line parallel to the solar equator [7] in combination with surface processes of diffusion and advection, has as a consequence a net transport of flux towards the poles that cancels the old polarity and reverses the sign of the poloidal field, setting the stage for the following cycle [5,6,8].

Because of its cyclic modulation of the heliospheric environment [9], Earth's magnetosphere [10], and the Sun's radiative output [11], the prediction of the solar cycle has commanded an increasingly large effort since the dawn of the space age [12]. Cycle predictions are typically classified into extrapolation methods, which use the mathematical properties of the sunspot data series to predict future levels of activity; precursor methods, which use different measurable quantities as a proxy to estimate the subsequent cycle's amplitude; and model-based predictions, which use the assimilation of data into models of the solar cycle to make predictions. There is, however, no consensus yet about the most effective method of cycle prediction, evidenced by nearly a hundred widely spread predictions for the amplitude of solar cycle 24 (whose prediction range spans all cycle amplitudes ever observed) [12,13].

One of the determinant factors shaping the nature of current prediction methods is the availability (or lack) of long-term solar records. For example, while most precursor methods are based on the logic that polar fields at solar minimum are the seed of the following cycle (first used to predict solar cycle 21 [14]), in reality most use geomagnetic activity measurements for predictions [13] due to the lack of polar field measurements before 1970. Another important limiting factor arises from the fact that both the sunspot record—which has long been regarded as one of the main indicators of solar activity and thus is used by most to calibrate and verify cycle prediction—and geomagnetic activity are solar global variables. This has resulted in cycle predictions dealing exclusively with the whole-Sun cycle amplitude while, in reality, hemispheric asymmetries of both the sunspot record [15,16] and the polar fields [17] suggest that the cycle in the northern and southern hemispheres are loosely coupled and should be predicted separately.

In this Letter, we take advantage of a recently standardized database of polar faculae measurements going back to the beginning of the 20th century (as a proxy for

 

the evolution of the polar magnetic flux) [18], in combination with a long-term homogeneous sunspot area database [19], to demonstrate the advantages of using the dipolar and quadrupolar moments of the solar magnetic field to make hemispheric predictions. Additionally, by extending the observed relationship between the polar field and the amplitude of the next cycle to a full century, we substantiate predictions based on the polar field [20–22]—currently inconspicuous among the many different predictions of solar cycle 24.

*Data.*—In this Letter we use a homogeneous database of sunspot areas [19], separated in northern and southern hemisphere sets, calculating the total hemispheric daily sunspot area [Fig. 1(a)]. Areas belonging to groups observed at the equator are not assigned to any of the two hemispheres. We remove high-frequency components by convolving our data series with a modified 24-month Gaussian filter [23], found to yield more consistent results while finding maxima and minima using different activity proxies than the traditional 13-month running mean.

Our magnetically calibrated polar faculae database [Fig. 1(b)] comes from a recent calibration and standardization [18] of four facular Mount Wilson Observatory (MWO) data reduction campaigns [24–27]. Consecutive campaigns were cross-calibrated using five year overlaps and validated using an automatic detection algorithm on intensity data from the Michelson Doppler Imager [28]. The resultant faculae database was calibrated in terms of polar magnetic field and flux using magnetic field measurements taken by the Wilcox Solar Observatory and SOHO/MDI (see Supplemental Material [29] for more details on our data sets).

*Hemispheric vs whole-Sun cycles.*—Following the current standard practice of making whole-Sun predictions, our first task is to study the relationship between the Sun's axial dipole moment at minimum (which is proportional to the unsigned average of the northern and southern polar magnetic fluxes) and the amplitude of the next cycle. We find them to be correlated [with a with a Pearson's correlation coefficient of $\rho = 0.69$ and $P = 96\%$ confidence level; see Fig. 2(a)]. However, a linear fit using least absolute residuals (LAR, which naturally gives less weight to possible outliers in the data set), shows a departure from the linear relationship one expects from the amplification of toroidal field out of poloidal field by differential rotation (an issue that does not affect cycles so far predicted using polar field measurements, i.e., 21–23). This deviation from linearity becomes more evident while looking at it from a hemispheric point of view [Fig. 2(b)], where a linear fit using LAR highlights the apparent existence of two separate branches. A comparison between the hemispheric and whole-Sun relationship shows that deviations using whole-Sun cycles are associated with a hemisphere falling outside the main branch.

*Solar magnetic moments and their relationship with irregularities in cycle shape.*—A qualitative assessment of hemispheric cycles and polar fluxes during the preceding minimum [Figs. 1(a) and 1(b) shows that off-branch hemispheric cycles [15S, 16N, 18N, and 20N, shown in Fig. 2(b) with triangular and star markers] are characterized by an extended multimodal maximum (as opposed to hemispheric cycles in the main branch, which generally show a peaked shape)—a characteristic that we quantify by dividing the cycle into rising, maximum, and decay phases and measuring the duration (width) of the maximum phase (see Supplemental Material [29]). Additionally, we find off-branch hemispheric cycles to be preceded by minima characterized by magnetic flux imbalance between the north and the south poles. Note that these cycles correspond to cycles for which only facular data are available,

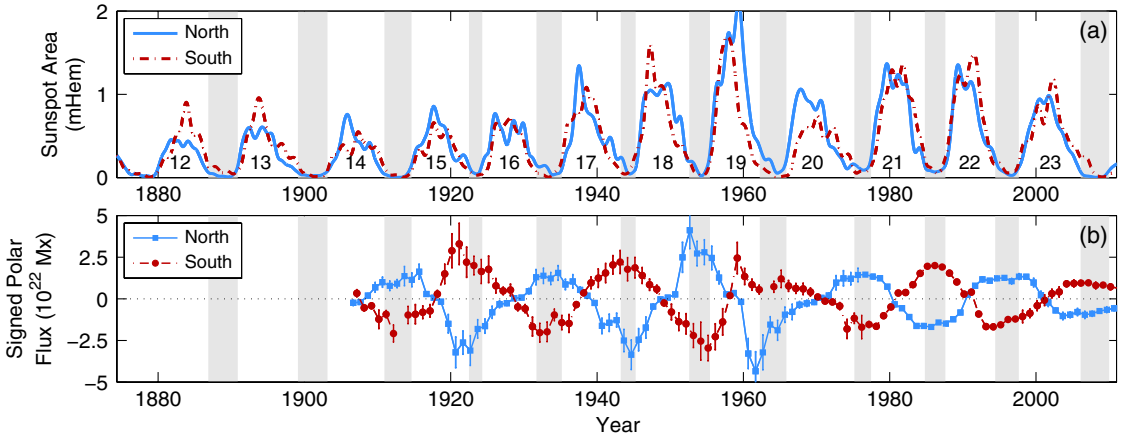


FIG. 1 (color online). (a) Smoothed daily sunspot area for the northern (solid blue line) and southern (dashed red line) hemispheres. (b) Polar flux (based on magnetic and polar faculae observations) for the northern (blue squares) and southern (red circles) hemispheres. Shaded areas indicate the duration of solar minimum defined as the period between points set at 15% of the amplitude of the corresponding bracketing cycle. Unless otherwise noted, all polar flux values used in this letter correspond to minimum averages.

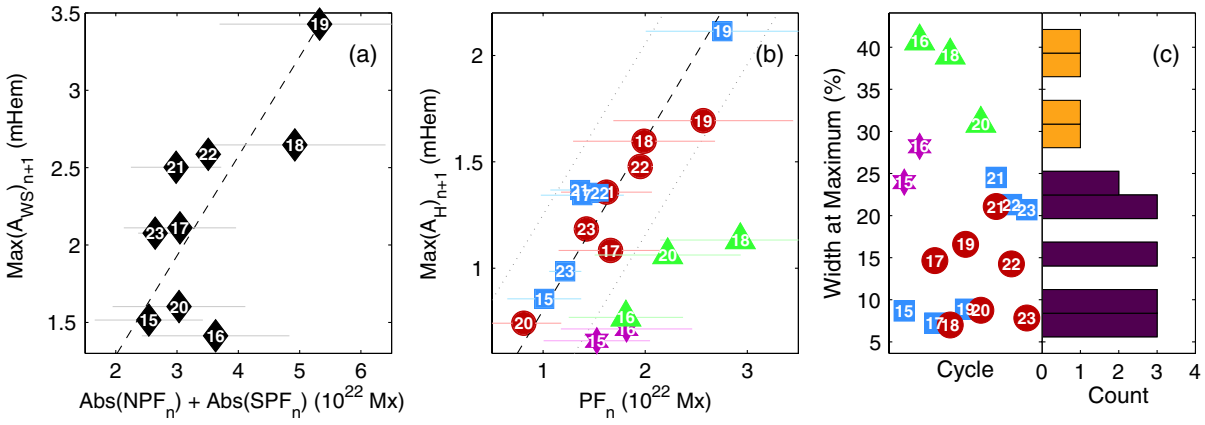


FIG. 2 (color online). (a) Average of the unsigned northern (NPF) and southern (PFN) polar fluxes (as an indicator of the Sun's dipole moment) at the minimum of cycle $n$ vs amplitude of the next whole-Sun cycle. Numbers denote the cycle being predicted. (b) Polar fluxes (PF) for the northern (blue squares and green triangles) and southern (red circles and magenta stars) hemispheres at the minimum of cycle $n$ vs amplitude of the next corresponding hemispheric cycle. Error bars are shown as faint horizontal lines. The dashed line in both panels corresponds to a linear fit using the least absolute residuals method. Numbers indicate the cycle being predicted. (c) Histogram of hemispheric width at maximum in units of cycle length. Peaked hemispheric cycles are denoted using blue squares (red circles) for the northern (southern) hemisphere. Cycles with an extended maximum are denoted using green triangles (magenta stars) for the northern (southern) hemisphere; markers in all hemispheric scatter plots have this same meaning. Histogram bars are colored to separate the bins which contain cycles belonging to the two different branches.

so we cannot rule out completely that these imbalances are caused by issues in the facular data. However, the strongest polar flux asymmetry in our data set (taking place around 1960) is also visible using MWO magnetograms as well [30]. This suggests that these asymmetries are real.

A histogram of hemispheric width at maximum (WaM) [Fig. 2(c)] shows how off-branch hemispheric cycles are consistently those with the highest values. Considering that sunspot cycles in our data set generally have only one off-branch hemisphere (or none), this means that sunspot cycles with hemispheres in separate branches are characterized by a strong asymmetry in shape. This hemispheric asymmetry is well correlated with the relative strength of the axial quadrupolar (QM) and dipolar (DM) moments during the preceding minimum [with a Pearson's correlation coefficient of $\rho = 0.8$ and $P = 99\%$ confidence level; Fig. 3(a)], calculated using the difference and average, respectively, of the unsigned northern and southern polar fluxes (see Supplemental Material [29] for more details).

Invoking recent high-resolution observations of the polar field, showing it to be concentrated in unipolar patches of magnetic field (in many cases of mixed opposite polarities) [31], we can propose a possible explanation of the relationship between a significant QM and

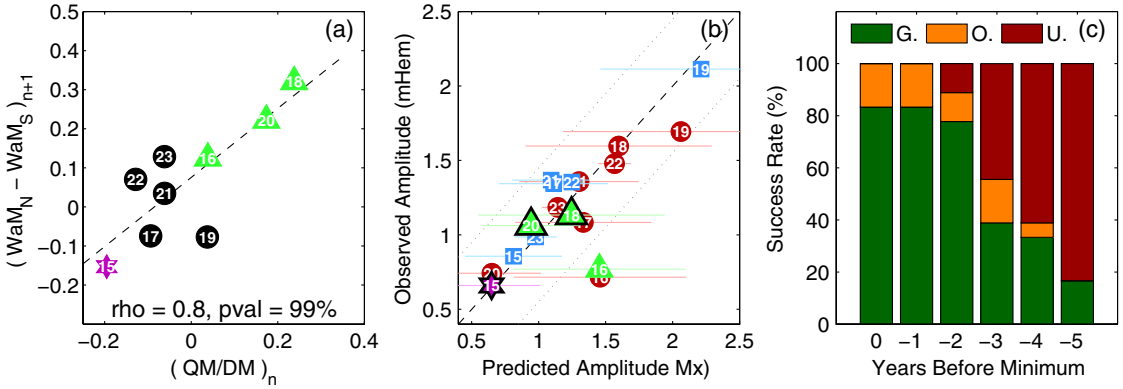


FIG. 3 (color online). (a) Ratio between the solar dipolar (DM) and quadrupolar (QM) moments at the minimum of cycle $n$ vs difference in cycle width at maximum. (b) Predicted vs observed cycle amplitude. Cycles with $|\mathrm{QM/DM}| \geq 16.5\%$ are predicted using the off-branch relationship (denoted with black outlines). Error bars are shown as faint horizontal lines. (c) Success rate of the prediction method when made using polar flux measurements taken at, or 1–5 years before, minimum. The lower section of each column (dark green) indicates predictions within the 99% confidence bounds, the middle section (light yellow) overestimated amplitudes, and the top section (red) underestimated amplitudes. See Supplemental Material [29] for the scatter plots used to create this figure.

hemispheric asymmetry: a significant QM means that while in one polar crown almost all poloidal field bundles are of the same polarity, in the other one there is a higher mixture of patches with opposite polarities. These conflicting bundles are wound independently by differential rotation, canceling and interacting with each other as the cycle progresses, resulting in a multimodal hemispheric cycle (with a lower amplitude than a smooth cycle would have), while in the other hemisphere the cycle turns out nice and sharp.

*Prediction of hemispheric cycles.*—We refine predictions based on the polar fields by taking advantage of the fact that QM-DM during minimum is a good indicator of whether one (and which) of the subsequent hemispheric cycles will have an extended maximum (and thus be off the main branch). We perform separate fits to the main and secondary branches [shown in Fig. 2(b)] and use an upper (lower) limit of QM-DM $\geq \mathrm{lim} = 16.5\%$ (QM-DM $\leq \mathrm{lim} = -16.5\%$) as criteria for choosing the relationship used for prediction of the northern (southern) hemispheric cycle. Our predictors become

$$\mathrm{Amp(PFN)}_{n+1} = \begin{cases} a_{\mathrm{mb}}\mathrm{PFN}_n & \frac{\mathrm{QM}}{\mathrm{DM}} \leq \mathrm{lim} \\ a_{\mathrm{sb}}\mathrm{PFN}_n & \frac{\mathrm{QM}}{\mathrm{DM}} > \mathrm{lim} \end{cases} \quad (1)$$

and

$$\mathrm{Amp(PFS)}_{n+1} = \begin{cases} a_{\mathrm{mb}}\mathrm{PFS}_n & \frac{\mathrm{QM}}{\mathrm{DM}} \geq -\mathrm{lim} \\ a_{\mathrm{sb}}\mathrm{PFS}_n & \frac{\mathrm{QM}}{\mathrm{DM}} < -\mathrm{lim}, \end{cases} \quad (2)$$

where $a_{\mathrm{mb}} = 0.802\,\mathrm{mHem}/10^{22}\mathrm{Mx}$ ($a_{\mathrm{sb}} = 0.425\,\mathrm{mHem}/10^{22}\mathrm{Mx}$) is the proportionality coefficient of the main (secondary) branch.

Considering that there is not a significant quadrupolar moment during the minimum of sunspot cycle 23 (QM − DM = 0.05), we use the main branch's relationship to predict an amplitude of $590 \pm 143$ $\mu$Hem (sunspot number $R = 36 \pm 9$) for the northern hemisphere and $664 \pm 108$ $\mu$Hem (sunspot number $R = 41 \pm 7$) for southern hemisphere in cycle 24 [Fig. 3(b)]. Together they give a maximum of $1254 \pm 251$ $\mu$Hem (sunspot number $R = 77 \pm 16$) for the amplitude of cycle 24, making cycle 24 one of the weakest cycles in the last hundred years, agreeing with other predictions based on the solar polar field [20,21].

To finalize, we study the efficacy of hemispheric predictions using polar flux measurements taken at, and before, solar minimum. Figure 3(c) shows a quantitative assessment of this performance in time. We consider the prediction to be accurate if it differs from the observed amplitude by less than our fit's 99% confidence bounds. In particular, we find predictions for solar cycle 24 to change only by 10% during the three years before minimum (from sunspot number $R = 85 \pm 10$ using values from 2005 to $R = 77 \pm 16$ at solar minimum in 2008); however, most minima in our database do not seem to stabilize as early. We find the method to perform well up to two years before minimum (with a success rate of 83% − 78%), after which the success rate drops dramatically.

*Concluding remarks.*—The results presented here (involving a full century of observations) demonstrate the power of solar polar fields during solar minimum as predictors of the amplitude of the next cycle (and do so in agreement with our theoretical understanding of the solar cycle). In particular, we show how polar flux becomes a better cycle predictor by taking advantage of the hemispheric polar fields to calculate both the dipolar and quadrupolar moments—the reason being that minima with significant quadrupolar moments lead to irregular hemispheric cycles with lower effective amplitudes than they would have if they were not irregular. We predict smooth hemispheric cycles for solar cycle 24 with amplitudes of $R = 36 \pm 9$ ($R = 41 \pm 7$) for the northern (and southern) hemispheres for a total whole-Sun amplitude of $R = 77 \pm 16$.

Our work paves the way for a new generation of precursor methods where the objective is no longer to find which variable yields the most accurate predictions, but rather how to make predictions better. One of the crucial points that needs to receive more attention is the timing of the solar cycle, both in terms of solar maximum (which is as important for long term planning as cycle amplitude) and solar minimum (considering that predictions based on the polar field are only accurate if made within two years of minimum). Another important issue is to broaden the concept of cycle prediction to include solar minimum conditions, in order to extend our predictive capability in time (ideally to more than one solar cycle).

Above all, our results add to the mounting evidence showing the solar poles to be a crucial link in the evolution of the solar cycle. We anticipate that Solar Orbiter, an ESA mission under development, by going out of the ecliptic and looking down on the poles will be able to uncover unknown details of the polar magnetic field evolution, thus considerably enhancing its understanding in the coming decade—specially in conjunction with the long-term full-Sun view of NASA's Solar Dynamics Observatory and the high-resolution observations of Solar-C of ISAS/JAXA.

We are thankful to Sami Solanki, María Dasi-Espuig, and María Navas-Moreno, and two anonymous referees for useful discussions and suggestions. This research is supported by the NASA Living With a Star Jack Eddy Postdoctoral Fellowship Program, administered by the UCAR Visiting Scientist Programs. Andrés Muñoz-Jaramillo is grateful to David Kieda for his support and sponsorship at the University of Utah. E. DeLuca was supported by Contract No. SP02H1701R from Lockheed Martin to SAO.

*amunoz@cfa.harvard.edu

[1] E. N. Parker, Astrophys. J. **122**, 293 (1955).
[2] E. N. Parker, Astrophys. J. **121**, 491 (1955).
[3] Y. Fan, Living Rev. Solar Phys. **6**, 4 (2009).
[4] P. Charbonneau, Living Rev. Solar Phys. **7**, 3 (2010).
[5] H. W. Babcock, Astrophys. J. **133**, 572 (1961).
[6] R. B. Leighton, Astrophys. J. **156**, 1 (1969).
[7] G. E. Hale, F. Ellerman, S. B. Nicholson, and A. H. Joy, Astrophys. J. **49**, 153 (1919).
[8] Y.-M. Wang, A. G. Nash, and N. R. Sheeley, Jr., Astrophys. J. **347**, 529 (1989).
[9] R. Schwenn, Space Sci. Rev. **124**, 51 (2006).
[10] T. Pulkkinen, Living Rev. Solar Phys. **4**, 1 (2007).
[11] V. Domingo, I. Ermolli, P. Fox, C. Fröhlich, M. Haberreiter, N. Krivova, G. Kopp, W. Schmutz, S. K. Solanki, H. C. Spruit, Y. Unruh, and A. Vögler, Space Sci. Rev. **145**, 337 (2009).
[12] K. Petrovay, Living Rev. Solar Phys. **7**, 6 (2010).
[13] W. D. Pesnell, Sol. Phys. **281**, 507 (2012).
[14] K. H. Schatten, P. H. Scherrer, L. Svalgaard, and J. M. Wilcox, Geophys. Res. Lett. **5**, 411 (1978).
[15] N. V. Zolotova, D. I. Ponyavin, R. Arlt, and I. Tuominen, Astron. Nachr. **331**, 765 (2010).
[16] A. A. Norton and J. C. Gallagher, Sol. Phys. **261**, 193 (2010).
[17] L. Svalgaard and Y. Kamide, Astrophys. J. **763**, 23 (2013).
[18] A. Muñoz-Jaramillo, N. R. Sheeley, Jr., J. Zhang, and E. E. Deluca, Astrophys. J. **753**, 146 (2012).
[19] L. A. Balmaceda, S. K. Solanki, N. A. Krivova, and S. Foster, J. Geophys. Res. **114**, A07104 (2009).
[20] K. Schatten, Geophys. Res. Lett. **32**, L21106 (2005).
[21] L. Svalgaard, E. W. Cliver, and Y. Kamide, Geophys. Res. Lett. **32**, L01104 (2005).
[22] A. R. Choudhuri, P. Chatterjee, and J. Jiang, Phys. Rev. Lett. **98**, 131103 (2007).
[23] D. H. Hathaway, Living Rev. Solar Phys. **7**, 1 (2010).
[24] N. R. Sheeley, Jr., Astrophys. J. **144**, 723 (1966).
[25] N. R. Sheeley, Jr., J. Geophys. Res. **81**, 3462 (1976).
[26] N. R. Sheeley, Jr., Astrophys. J. **374**, 386 (1991).
[27] N. R. Sheeley, Jr., Astrophys. J. **680**, 1553 (2008).
[28] P. H. Scherrer, R. S. Bogart, R. I. Bush, J. T. Hoeksema, A. G. Kosovichev, J. Schou, W. Rosenberg, L. Springer, T. D. Tarbell, A. Title, C. J. Wolfson, I. Zayer, and MDI Engineering Team, Sol. Phys. **162**, 129 (1995).
[29] See Supplemental Material at http://link.aps.org/supplemental/10.1103/PhysRevLett.111.041106 for data filtering and processing details.
[30] Leif Svalgaard (private communication).
[31] D. Shiota, S. Tsuneta, M. Shimojo, N. Sako, D. Orozco Suárez, and R. Ishikawa, Astrophys. J. **753**, 157 (2012).